INVESTIGATION OF STRAINS IN MICROREGIONS OF POLYCRYSTALS WITH THE AID OF PHOTOELASTIC COATINGS

A. Ya. Aleksandrov, L. A. Krasnov and V. A. Kushnerov

Zhurnal Prikladnoi Mekhaniki i Tekhnicheskoi Fiziki, Vol. 8, No. 3, pp. 76-82, 1967

Due to its many advantages (small base of measurements, convenience in use, possibility of recording the entire strain field, reliability in measuring both the elastic and plastic strains, etc.) the photoelastic method has found a wide application as a means of measuring strains in various structural elements [1-4]. The method was used in several studies [3-9] of strain fields in metal grains, i.e., so called "microstrains."

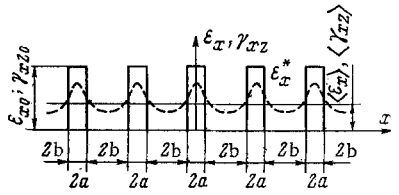

Fig. 1

However, the quantitative measurement of strains presents certain problems associated with the resolving power and accuracy of this method, since these characteristics determine the size of deformed regions and the character of deformation for which the results of measurements may be regarded as sufficiently reliable.

These and certain other problems associated with the use of the photoelastic method for the quantitative determination of microstrains in polycrystals are analyzed in this article.

Experimental techniques are discussed and recommendations are made regarding the means of increasing the sensitivity of measurements by using a compensation method of measuring the optical difference of the beam of light passing through a photoelastic coating and photographically recording the results. Some results of a study of strains in metal grains are reported, the size of regions in which strains of 0.1% were successfully measured being on the order of 10^{-2} mm. A method of studying residual stresses in separate grains of specimens after macrouniform plastic deformation is described and the results cited.

1. Resolving power of the method. Choosing the correct thickness of photoelastic coatings. Generally speaking, strains in a photoelastic coating are uniformly distributed across its thickness, and their averaged values measured with the aid of normal translumination of the coating are not equal to strains on the specimen surface. The resulting error decreases with decreasing coating thickness, this being accompanied by a corresponding increase in the resolving power of the method.

However, the extent to which the coating thickness can be reduced is limited by the sensitivity of the instrument measuring the optical path difference. If therefore one has to use coatings whose thickness is larger than the size of strain concentration regions, it is first necessary to establish whether these regions can be differentiated, i.e., to estimate the resolving power of the method. If the resolving power is sufficiently high, the experimental error can be estimated by the known methods [10,11]. It may be assumed that this error is relatively small if the coating thickness is not larger than the size of regions in which the strain is constant or varies linearly and if the distance (from the edge of such a region) at which a measurement is carried out is not smaller than the coating thickness.

Let us consider the problem of determining the resolving power in the case when the strain distribution along an axis in the specimen plane is represented by a Π-shaped graph shown as a solid line in Fig. 1. Such a distribution may occur if the strains are due to the formation of slip bands $2a$ wide, with the interband spacing equal to $2l$. Axes x and z are, respectively, normal and parallel to the band direction; γ_{xz} denotes the shear strain; $l = a + b$. A similar strain distribution will be obtained in the case of a specimen extended in the direction of the x axis and having a system of cracks ($2a$ wide, spaced at $2l$ intervals) normal to this axis. Let us obtain a solution for a specimen of this kind.

Let us assume that both the specimen and the coating work under plane strain conditions and that the coated portion of the specimen surface is not bent. The boundary conditions for the coating have the following form: at y = c, $\sigma_y = 0$, $\tau_{xy} = 0$; at y = 0, V = const, $\varepsilon_x = \varepsilon_{x_0}$ (along segments $2a$); at y = 0, $\varepsilon_x = 0$ (along segments 2b). Here σ_y and τ_{xy} are stress components in the coating, c is the coating thickness, V is the displacement along the y axis (which is normal to the coating plane).

Using the known solution of the plane problem of the theory of elasticity in series, we find the strain $\varepsilon_x(xy)$ in the coating.

When the coating is transluminated in the direction of y axis, one measures the averaged (over the coating thickness) strain

$$\varepsilon_x^* = \frac{1}{c}\int_0^c \varepsilon_x\, dy. \qquad (1.1)$$

Substituting the expression found for ε_x in (1.1), we obtain

$$\varepsilon_x^* = \varepsilon_{x0}\left[\varphi + \frac{2}{\pi}\sum_{n=1}^{n=\infty}\frac{k_n}{n}\sin n\pi(1-\beta) + \cos n\pi\frac{x}{l}\right],$$

$$k_n = \frac{2}{u}\Big[(1-u^2)(2u+\operatorname{sh}2u) + 2m(1+m)\,u\operatorname{ch}u - 2m(1+m)\operatorname{ch}u\Big]\times$$
$$\times\Big[[4-(1-m)^2]\operatorname{ch}2u + 2(1+m)^2u^2 + (1-m)^2 + 4\Big]^{-1},$$

$$\beta = \frac{b}{l},\quad \varphi = \frac{a}{l},\quad \gamma = \frac{c}{l},$$

$$m = \frac{\mu}{1-\mu},\quad l = a+b,\quad u = n\pi\frac{c}{l}. \qquad (1.2)$$

Here μ is the Poisson ratio of the coating material.

As the coating thickness increases, the measured strain ε_x^* approaches the average value $\langle\varepsilon\rangle = \varepsilon_{x_0}\varphi$. When the coating thickness is reduced, ε_x^* (dashed curve in Fig. 1) approaches the strain ε_x on the specimen surface. The resolving power of the coating will be considered as sufficiently high for the case under consideration, if it is possible to reveal nonuniformity of strain of the specimen studied, i.e.,

$$\max\varepsilon_x^* - \min\varepsilon_x^* \geqslant R\Delta_0. \qquad (1.3)$$

Here $\max\varepsilon_x^*$ and $\min\varepsilon_x^*$ denote the maximum and minimum values of strain, R is the stress-optical coefficient of the material, and Δ_0 is the accuracy of measuring the optical path difference; when the fringe counting method is used $\Delta_0 = 0.5\lambda$, while using compensators gives $\Delta_0 \approx 0.01\lambda$, where λ is the wavelength of the monochromatic light employed. Let us rewrite condition (1.3) in the form

$$\langle\varepsilon\rangle r \geqslant R\Delta_0 \qquad [r = (\max\varepsilon_x^* - \min\varepsilon_x^*)/\langle\varepsilon\rangle]. \qquad (1.4)$$

Values of the resolving power coefficient of the coating r (which depend on the coating thickness and the character of deformation of the specimen) are plotted in Fig. 2.

In the case when the strain distribution corresponds not to a system of parallel cracks but to a single crack, analogous formulas and estimates are obtained with the aid of results of [11].

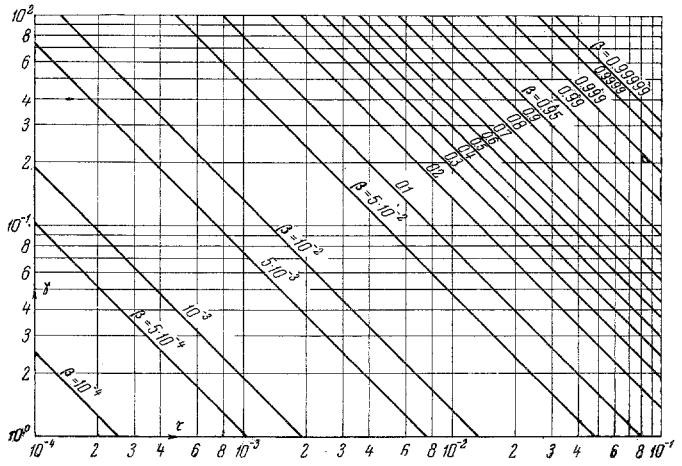

Fig. 2

2. Experimental technique. The experimental apparatus (Fig. 3) was based on a standard MIM-5 metallographic microscope, to the optical system of which were added a polarizer P, an analyzer A and, when necessary, quarter-wave plates which give an optical path difference equal to a quarter of the wavelength λ of the nonochromatic light used. The specimens were strained in tension on a special tensile machine with a spring dynamometer.

A special mechanical immersion compensator was constructed for measuring the optical path difference of the coating. The working part of this device is a sensitive plate 1 made of an optically active material. The plate, whose ends are attached to a steel bracket 2, is extended with the aid of a micrometer screw 3 whose scale is used to measure the optical path difference. The scale of such a compensator is practically linear which simplifies the calibration of the instrument and its operation. The compensator is mounted so that the sensitive plate (lying flat against the coating) covers the entire working region of the specimen. The gap between this plate and the coating is filled with an immersion fluid to eliminate the intereference background [12]. A turntable mounted on the microscope stage makes it possible to rotate the loading mechanism with the specimen 5 (whose cross section is shown in Fig. 3) and the compensator relative to the microscope for determining the isocline parameter, and to rotate the compensator relative to the specimen for measuring the optical difference of the light passage. The order of interference fringes produced by the apparatus shown in Fig. 3 depends on the optical path difference of the model and of the compensator and on the relative orientation of the optical axes of the coating and the compensator. If the compensator axes coincide with the direction of principal strains in the coating and, at the same time, are at an angle of 45° to the polarizer axis, the real fringe order n for the coating can be calculated from the formula

$$n = n^* \pm \delta / \lambda. \qquad (2.1)$$

Here n^* is the fringe order of the pattern recorded on a photoplate when the coating and the compensator are simultaneously transluminated, δ denotes the optical path difference of the compensator, and λ is the light wavelength. The "plus" sign in (2.1) is retained in cases when the compensator is operated "for subtraction," i.e., when compensator axes coincide with specimen axes of the opposite sign.

In the case of an apparatus in which the compensation is applied over the entire field of a model, conditions under which formula (2.1)

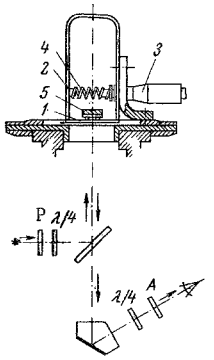

Fig. 3

is valid can be satisfied only at isolated points lying on a single-parameter isocline. Using the results of [13] relating to measurements under conditions of misalignment of the model and compensator axes, one can show that if the misalignment angle does not exceed 10°, the measurement error will be less than 6%. This makes it possible to carry out the compensation (accurate to an acceptable degree) simultaneously over any large region of a model in which the isocline parameters do not differ by more than 20°. The results of compensation are recorded on a photoplate; this is done by taking several successive photographs for various readings of the compensator whose axes are oriented in accordance with the average isocline parameter of the region studied. The real (fractional) fringe order is calculated from (2.1) accurate to a degree cited above. Example of interference fringe patterns obtained with the application of compensation over the field studied are shown in Fig. 4.

The photoelastic coatings were applied to polished and degreased specimens whose surface were sometimes etched to reveal their microstructure. The coating material consisted of an ED-6 type resin, a hardener (maleic anhydride, 33% of the resin weight) and a plasticizer (dibutylphthalate, 12% of the resin weight). To obtain a coating of a required thickness, a specimen with a liquid coating was pressed

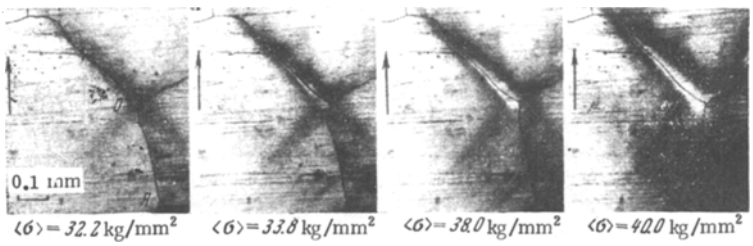

Fig. 4

against calibrated wire spacers placed on a polished glass plate. To prevent adhesion, the glass plate was previously flooded several times with a 0.5% solution of cellulose triacetate in methyl chloride and

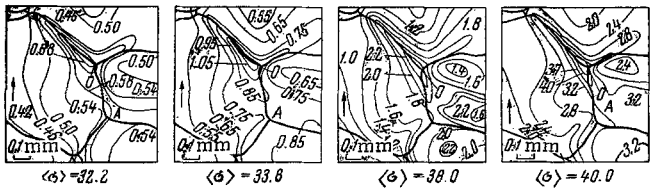

Fig. 5

dried in a dustproof thermostat, first at room temperature and then at 50–60° C. The resin coating was polymerized by a 6 hour treatment at 140° C after which the coated specimen was separated from the glass plate. In this way coatings of a thickness ranging from 0.01–0.05 mm (±0.001 mm) were obtained. The stress-optical coefficients of the coatings were determined by tests carried out in the elastic range on the actual specimens. For the calibration in the plastic strain range special specimens were prepared for tests using both transmitted and refracted light.

The following procedure was followed in selecting the photoelastic coating thickness that would ensure the required resolving power of the method. Results of preliminary experiments on analogous specimens were used tentatively to determine the minimum size of the strain concentration regions and the possible distances between these regions. It was then assumed in the first approximation that the strain distribution is represented by a Π-shaped graph, after which the maximum admissible coating thickness for the observation of strain regions of this size was calculated from (1.2). Actually, the coating thickness in the experiments described below was smaller than the values obtained by the method outlined above. In some cases the error associated with the influence of the coating thickness was estimated.

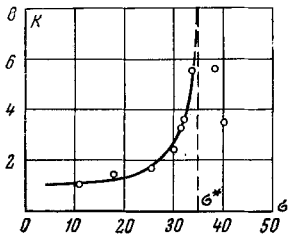

Fig. 6

3. Investigations of microstrains in high-quality E3 and C7 steel specimens in tension. The cross section of the gauge portion of experimental tensile steel specimens was 4 × 1.2 mm. To obtain large grains, the specimen blanks were annealed for 5 hr at 1200° C, after which the pertinent properties of high-quality E3 and C7 steel were: grain size 0.7 and 0.5 mm, the proportionality limit 34.4 and 49.0 kg/mm² and the conditional yield point 38.9 and 62.9 kg/mm².

The strain distribution in the specimen gage portion was studied at several stress levels corresponding to the elastic and elastic-plastic deformation. At each stress level up to seven photographs were taken at various readings of the compensator scale which made it possible to obtain strain data for the entire working field of the specimen.

The results obtained are exemplified by photographs taken for high-quality E3 steel specimens at nominal stresses 32.2, 33.8, 38.0 and 40.0 kg/mm² (with the compensator scale reading, respectively, 0.15, 0.22, 0.48 and 0.86 of the wavelength of the light employed) and reproduced in Fig. 4. Both the interference fringes (dark regions) and grain boundaries (retouched for the sake of clarity) are shown in these photographs; the direction of the applied tensile load is indicated by arrows. After processing photographs of this kind, we obtained values of the difference of the principal strains in the working field of a given specimen at all the stress levels studied. Typical results are reproduced in Fig. 5 showing the lines $\varepsilon_1 - \varepsilon_2 = \text{const}$ which characterize the distribution of the difference of principal strains (in percent) at the above cited stress levels; grain boundaries are also shown in this figure. The nonuniformity of deformation in microregions was measured in terms of the strain concentration coefficient

$$k = \frac{(\varepsilon_1 - \varepsilon_2)_{\max}}{\langle(\varepsilon_1 - \varepsilon_2)\rangle}. \qquad (3.1)$$

Here $(\varepsilon_1 - \varepsilon_2)_{\max}$ and $\langle\varepsilon_1 - \varepsilon_2\rangle$ denote, respectively, the maximum measured and the average difference of principal strains on the specimen surface.

The nonuniformity of strain in high-quality E3 steel specimens became noticeable from a nominal stress $\langle\sigma\rangle = 17.6$ kg/mm². For instance, the strain concentration coefficient at this nominal stress level calculated from (3.1) for point O, at which three grain boundaries meet (Fig. 5), was 1.32. With increasing load k continued to increase (Fig. 6); the regions of intense deformation at nominal stresses of up to 40 kg/mm² were located near the grain boundaries and, more often than not, did not intersect the grains. (Henceforth the symbol σ* used in Fig. 6 will denote the proportionality limit.) In isolated cases (see, e.g., the grain on the left side of boundary OA in Fig. 4) interference fringes resembling slip lines were observed in the grain interior of specimens tested at lower stress levels.

Fig. 7

In the later loading stages (when the strains in the grain-boundary regions were $(\varepsilon_1 - \varepsilon_2) > 6.0\%$) the heavy deformation zones extended to the grain interior. For instance, interference fringes corresponding to a strain difference of 6.6% are shown in Fig. 7, where the specimen edge can be seen on the left side of the photograph. It should be noted that at strains larger than 3.5% the magnitude of the experimental error was increased due to stress relaxation in the coating.

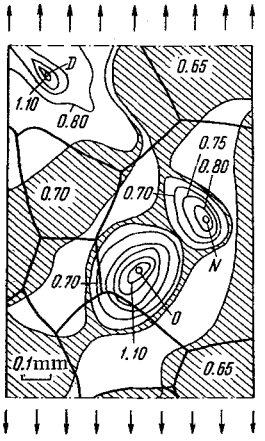

Fig. 8

The effect of this factor is negligible, however, if the measurements are carried out in a sufficiently short time.

In the case of a high-quality E3 steel specimen which before testing showed evidence of twinning, strain concentration was observed near the twin boundaries inclined to the longitudinal axis of the specimen (tested at

$\langle\sigma\rangle$ = 19.8 kg/mm^2) at an angle approaching 45°. Twin boundaries at substantially different angles to the specimen axis had no noticeable influence on the character of strain distribution at nominal stresses lower than the proportionality limit.

In the case of C7 steel specimens the nonuniformity of deformation became noticeable starting at $\langle\sigma\rangle$ = 40 kg/mm^2. The strain distribution in one of such specimens at $\langle\sigma\rangle$ = 60 kg/mm^2 is shown in Fig. 8, where crosshatched areas indicate regions of $(\varepsilon_1 - \varepsilon_2)$ = const. The strain concentration zone centered at point O in Fig. 8 was observed at $\langle\sigma\rangle$ = 40 kg/mm^2; as the load was increased, this zone grew in a direction at about 45° to the longitudinal specimen axis. At $\langle\sigma\rangle$ = 53 kg/mm^2 a new strain concentration center appeared at point N from which the strain concentration zone grew toward point D. Most of the C7 steel specimens deformed in a similar way. However, some specimens in the early loading stages behaved like high-quality steel specimens, i.e., favorably oriented grain boundaries acted as the centers of strain concentration.

4. Strain concentration near small radius holes. It is known that the structure of real crystalline solids affects the stress concentration coefficients during deformation in the vicinity of holes of a small radius comparable to the grain size [14]. We therefore carried out an experimental study of strain concentration in tensile high-quality E3 steel specimens with a circular hole. The specimen dimensions and values of the stress concentration coefficient k_m (equal to the ratio of the maximum stress

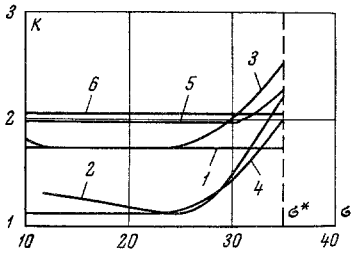

Fig. 9

at the hole edge to the average stress at infinity) for a homogeneous isotropic elastic material [15] are given below.

Specimen no.	1	2	3	4	5	6
Gauge portion width	6.94	3.94	8.98	9.04	8.96	8.85
Hole diameter	1.20	1.64	1.67	2.53	3.36	6.20
Coefficient k_m	3.04	3.79	3.05	3.25	3.54	—

The corresponding strain concentration coefficients k determined by experiment at various stress levels ($\langle\sigma\rangle \leq \sigma^*$) for points on the hole edge located on the diameter normal to the direction of loading are reproduced in Fig. 9, where the stress values correspond to the stress in the weakened specimen cross section and the numerals indicate the specimen number. In tests at stresses (in the weakened specimen cross section) equal to about 16 kg/mm^2 strain concentration was observed at other points on the hole edge, where the edge was intersected by grain boundaries inclined at approximately 45° to the longitudinal specimen axis. Increasing the load to the level of σ^* led to intense deformation in all the grain boundary regions (irrespective of the presence of a hole), and the increase in k recorded for specimen Nos. 2, 3 and 5 at higher loads (Fig. 4) is attributable to the influence of grain boundaries in the vicinity of the hole.

5. Investigation of residual stresses in steel grains after previous plastic deformation. The residual stresses in steel grains were determined by a method which involved cutting a specimen with a photoelastic coating into small segments. High-quality E3 steel sheet specimens in the as received condition (i.e., with a coarsely granular structure) measuring 10 × 80 × 0.3 mm were plastically deformed on a tensile machine and then coated with a photoelastic film 0.14 mm thick; a number of specimens were kept in the undeformed state for comparison. To obtain a more uniform stress state (approaching that in the specimen surface layers) across the specimen thickness, each specimen was chemically etched to a thickness of 0.15–0.20 mm, after which it was cut (by chemical etching) into 10–14 segments held together by the photoelastic coating. The width of these segments was then reduced by etching to 0.5–0.7 mm. The method of marking out the specimens for etching is shown in Fig. 10 where portions removed by etching are indicated by cross-hatching; the remaining specimen portions were coated with a protective nitrate film, the process of etching being periodically interrupted to reapply the protective coating.

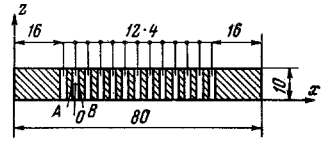

Fig. 10

Strain fields produced in one of the segments at three stages of the etching operation (corresponding to three different widths of the segment) are shown in Fig. 11. These strains are associated with the elastic component of the residual stresses in the specimen, it being assumed that the stress relaxation (due to metal removal) takes place in the elastic range. The strain magnitude along lines $(\varepsilon_1 - \varepsilon_2)$ = = const is given in percent, thick lines delineating the grain boundaries. The segment width AB is oriented along the parent specimen axis. The strain values given in Fig. 11 were calculated from data on the optical path difference in the photoelastic coating without correcting for errors made in measurements near the segment edges (due to nonuniform deformation of the coating across its thickness) and errors associated with thermal stresses produced during the polymerization (due to different thermal expansion coefficients of the steel and the coating material). The latter error is insubstantial, if the distance between the segment edge and the field where the measurements are carried out is not smaller than four coating thicknesses. An approximate correction [10] of the results was made on the assumption that the actual distribution of residual elastic strains along AB was close to uniform. The error due to the fact that the strain distribution is not in fact uniform can be reduced by further decreasing the segment width (by etching) and estimated by comparing results obtained at various etching stages.

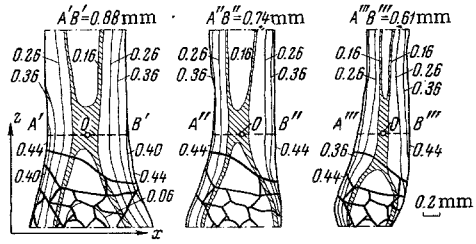

Fig. 11

REFERENCES

1. A. Ya. Aleksandrov, "A possible application of the photoelastic method in studies of plane elastic-plastic problems," Tr. Novosibirsk. in-ta inzh. zh.-d, transporta, no. 8, 1952.

2. A. Ya. Aleksandrov and M. Kh. Akhmetzyanov, "Investigation of elastic-plastic problems with the aid of photoelastic coatings," PMTF, no. 6, 1961.

3. A. Ya. Aleksandrov and M. Kh. Akhmetzyanov, "Investigation of plane elastic-plastic problems by the photoelastic method," Proceedings of the II All-Union Conference on Theoretical and Applied Physics, Izd-vo Nauka, vol. 3, 1966.

4. A. Ya. Aleksandrov, M. Kh. Akhmetzyanov and L. A. Krasnov, "Investigation of elastic-plastic elements by the photoelastic method," Tensometric Methods and Instruments [in Russian], no. 5, Izd. Gos. in-ta. n-tekhn. informatsii, 1964.

5. B. A. Kuznetsov, "Polarization method of investigating small plastic strains," Zavodsk. laboratoriya, no. 5, 1957.

6. K. Kavata, N. Tokata and S. Khasimoto, "Investigation of elastic-plastic strains in coarsely crystalline metals by the method of optically active coatings," Oyo Buturi, vol. 31, no. 10, 1962.

7. F. Zandmann, "Mesures photoélastiques des deformations cristallines dans les métaux," Rev. métallurg., no. 8, 1956.

8. P. I. Polukhin, Yu. D. Zheleznov and G. G. Grigoryan, "Application of the method of optically sensitive coatings in studies of plastic deformation of polycrystalline metals," Fiz. metallov i metallovedenie, vol. 15, no. 6, 1963.

9. B. A. Kuznetsov, "Initial stages of plastic deformation of polycrystals," Dokl. AN SSSR, vol. 159, no. 1, 1964.

10. L. A. Krasnov, "Accuracy of measurements with the aid of photoelastic coatings," Tensometric Methods and Instruments, Vol. 5 [in Russian], Izd. GOSINTI, 1964.

11. L. A. Krasnov, "Accuracy of strain measurements with the aid of photoelastic coatings," Proceedings of the All-Union Conference on the Polarization-Optical Methods of Stress Measurements (Leningrad, 1964) Izd. Leningrad. un-ta, 1966.

12. L. A. Krasnov, "Measuring the optical path difference in studies by the photoelastic method," Tr. Novosibirsk. in-ta zh. d. transporta, no. 24, 1961.

13. A. Ya. Aleksandrov and L. A. Krasnov, "Electric compensator for measuring the optical path difference in studies by the photoelastic method," Izv. AN SSSR, Mekhanika i mashinostroeni, no. 1, 1959.

14. H. Neuber, Stress Concentration [Russian translation], Gostekhizdat, 1947.

15. G. N. Savin, Stress Concentration Around Holes [in Russian], Gostekhizdat, 1951.

2 August 1966 Novosibirsk